Nanoscience and Nanotechnology Letters
Vol. 9, 24–29, 2017

Effect of Structure and Material Variation of Focus Ring for Enhanced Etch Resistance

Kyung Chae Yang[1, †], Sung Woo Park[1, †], Ho Seok Lee[2], Dong Woo Kim[1], and Geun Young Yeom[1, 2, *]

[1] *School of Advanced Materials Science and Engineering, Sungkyunkwan University, 2066, Seobu-ro, Suwon, South Korea*
[2] *SKKU Advanced Institute of Nano Technology (SAINT), Sungkyunkwan University, 2066, Seobu-ro, Suwon, South Korea*

For the reactive ion etching of nanoscale semiconductor devices, it is very important to maintain uniform etch rates over the wafer surface to the near-edge of the wafer, and, for the enhanced etch uniformity, a focus ring which surrounds the silicon wafer is used. However, due to the continuous etching (that is, eroding) of the focus ring during the use of the etch system, the wafer etch characteristics are drifted and particles are generated on the wafer surface. In this study, the effects of structure and materials of the focus ring on the etch characteristics of the focus ring were investigated to improve the lifetime of the focus ring. Among the materials investigated such as polytetrafluoroethylene (PTFE), alumina (Al_2O_3), zirconia (ZrO_2), quartz (SiO_2), and yttrium oxide (Y_2O_3), the material which as the lowest dielectric constant exhibited the lowest etch rate. In addition, when the materials were fabricated to contain more air gap in the structure, therefore, to have less overall dielectric constant, less etching of the materials was obtained. The lowest etch rates observed for the material with the lowest dielectric constant and for the structure with the lowest dielectric constant structure were related to the lowest sheath potential developed over the focus ring materials, therefore, the lowest ion bombardment energy to the focus ring surface. It is believed that, by designing the lowest dielectric material/structure as the focus ring body with the lowest sputter yield materials as the surface materials of the focus ring, the longest lifetime of the focus ring for nanoscale semiconductor processing could be achieved.

Keywords: Focus Ring, Nanoscale Semiconductor, Etch Resistance, Plasma Sheath, Focus Ring Lifetime.

1. INTRODUCTION

In manufacturing semiconductor devices, various plasma etching tools such as inductively coupled plasma (ICP) etcher, capacitively coupled plasma etchers, etc. are widely used.[1, 2] In these etchers, as the semiconductor device size is decreased to deep nanoscale, not only the good uniformity to the near-edge of the wafer but also the decreased nanoparticle formation during the etching has become important. To improve the etch uniformity over the wafer area, a focus ring, which is installed around the edge of the wafer for more uniform plasma all over the wafer area by extending the plasma above the wafer edge to the focus ring, is generally used.[3–5] Also, the use of the focus ring is known to improve the azimuthal uniformity of power deposition in the etcher by confining the electric discharge in the chamber.[6, 7] However, when the etching process is performed, not only the wafer to be etched but also the focus ring is continuously exposed to the energetic reactive ions, therefore, the focus ring exposed to the plasma is also etched and eroded.[8] As the focus ring is a consumable part, the focus ring needs to be exchanged periodically with a new one whenever the accumulated time of the etching process is longer than 500 hours due to the change of plasma characteristics, the change of uniformity, and increase of particles on the wafer which is caused by severe erosion of the focus ring.[9, 10] To improve the lifetime of the focus ring and to decrease the particle issue, considerable work and research has been done to develop more etch resistant focus ring by developing materials with less sputter yield and more reactive etch resistance.

For the improvement of the lifetime of the focus ring, the improved material characteristics such as lower reactivity and lower sputter yield are important. However, for the plasma etching, due to the electrical characteristics of a plasma, a plasma sheath is developed on the focus ring surface[11] and the formation of a smaller plasma sheath voltage in the plasma sheath over the focus ring can be

*Author to whom correspondence should be addressed.
†These two authors contributed equally to this work.

 1941-4900/2017/9/024/006 doi:10.1166/nnl.2017.2296

equally important in increasing the lifetime of the focus ring because it can decrease the etch rates to the etch gases significantly by decreasing the reactive ion energy bombarding the focus ring. Therefore, in this study, to change the voltage developed in the plasma sheath on the focus ring while keeping the same ion bombardment energy to the wafer surface, materials and structure of the focus ring were varied while keeping the surface of the focus ring with the same material (SiO_2) to investigate the effect of material and structure of the focus ring body on the erosion characteristics of the focus ring by changing the dielectric characteristics of the focus ring body. The change of dielectric constant of the focus ring body by the varying the structure (for example, by adding air gap) and by using different materials will change the impedance of the focus ring and it will change the plasma sheath voltage on the focus ring during the reactive ion etching, and which will affect the lifetime of the focus ring by varying the ion energy to the focus ring surface.

2. EXPERIMENTAL DETAILS

A schematic diagram of the experimental setup for the etch experiment of focus ring material and structure is shown in Figure 1. A cylindrical anodized aluminum chamber with an inner diameter of 650 mm and a height of 400 mm ICP reactor has been used in this study. To the top ICP source, 13.56 MHz rf power was connected through a matching network to form high density plasmas and, to the bottom electrode, 12.56 MHz rf power was applied through a separate matching network to generate bias voltage, that is, ion bombardment energy to the wafer. The reactive gases were evenly distributed in the vacuum chamber by using a multi-hole shower ring located along the periphery of the chamber as shown in Figure 1. The base pressure less than 5×10^{-6} Torr was routinely achieved by using

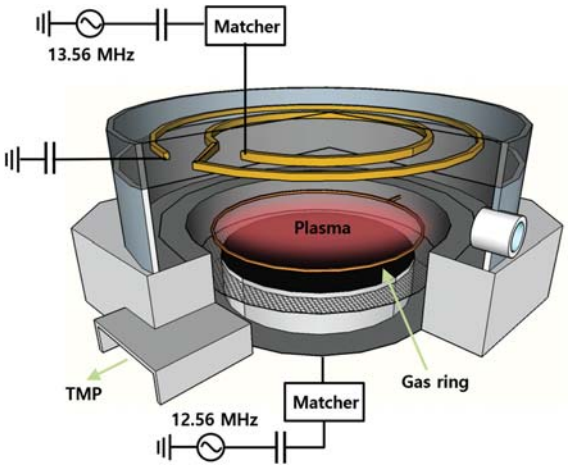

Fig. 1. Schematic diagram of the ICP system used in this study for the etch experiment of focus ring.

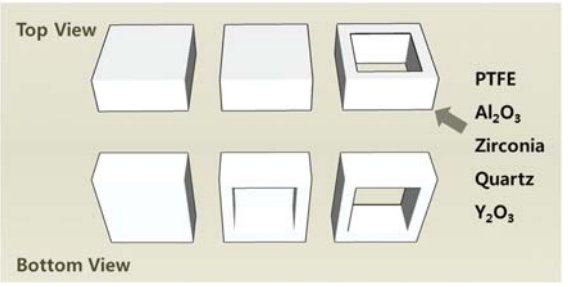

Fig. 2. Structures and materials used as the focus ring in the experiment. Three different structures including an air gap with the dielectric constant of 1.0 were used and five different materials having different dielectric constants such as PTFE, Al_2O_3, ZrO_2, SiO_2, and Y_2O_3 were used.

a turbomolecular pump (Edwards STP-A3503) backed by the dry pump (Alcatel ADP 122P).

To change the dielectric constant of the materials, three different structures of material containing an air gap as shown in Figure 2 were used. 1 cm × 1 cm × 0.5 cm (height) material consisted of all solid material, 1/2 of inside material filled with an air gap, all of inside material filled with air gap were used. As the material itself, five different materials having different dielectric constants such as polytetrafluoroethylene (PTFE), alumina (Al_2O_3), zirconia (ZrO_2), quartz (SiO_2), and yttrium oxide (Y_2O_3) were investigated. Table I shows dielectric constant of materials using in this study. For the focus ring etch experiment, to investigate the effect of different dielectric constant, that is, different capacitance of the focus ring by varying structures and materials, the surface of the focus ring was covered with the same material (not to have different reactivity and sputter yield for different focus ring materials/structures), that is, with 400 nm thick SiO_2 film deposited glass wafer. This 400 nm thick SiO_2 film was patterned by 2.0 μm thick photoresist to measure the etch depth after the etch experiment. The focus ring etching was carried out with Ar (200 sccm)/CF_4(45 sccm)/O_2 (30 sccm), at the processing pressure of 75 mTorr, ICP power of 800 W, and the bias power of 1200 W for all experiments.

The etch rates of SiO_2 samples mounted on the three types of structures/five different materials were estimated using a field emission scanning electron microscopy (FE-SEM, Hitachi S-4700) by taking cross-sectional

Table I. Dielectric constant of materials used in the experiment.

Material	Dielectric constant ($\varepsilon/\varepsilon_0$)	Refs.
Aluminum oxide, Al_2O_3	9∼11	[12, 18]
Yttrium oxide, Y_2O_3	9∼15	[13, 18]
Zirconia, ZrO_2	22∼45	[12, 14]
Polytetrafluoroethylene (PTFE)	2∼2.1	[15, 19]
Air	1	[16]
Si	11.7	[17]
Quartz, SiO_2	3.9∼4	[17, 18]

Table II. SRIM input parameters for various dielectric materials. ρ is the bulk material density, E_D is the bulk atom displacement energy and E_L is the lattice energy, and U_0 is the surface atom binding energy. Each value was achieved in the reference.

Mat.	ρ (g/cm^3)	E_D (eV)	E_L (eV)	U_0 (eV)	Refs.
Al_2O_3	3.99	Al:25 O:25	Al:3 O:3	Al:3.4 O:2.1	[20, 21]
ZrO_2	6.10	Zr:40 O:40	Zr:7.70 O:6.74	Zr:6.31 O:5.89	[22–25]
Quartz	2.65	Si:21 O:22	Si:2.1 O:2.2	Si:3.1 O:3.2	[26, 27]
Y_2O_3	5.03	Y:25 O:28	Y:3 O:3	Y:4.2 O:2	[21, 28, 29]

images of SiO_2 with the photoresist. To investigate the effect of focus ring material itself on the etch resistance which was not considered in this experiment, the stopping and range of ions in matter (SRIM) simulation was conducted to investigate the sputter yield $\langle S \rangle$ of PTFE, Al_2O_3, ZrO_2, SiO_2, and Y_2O_3 using energetic Ar ions. The type of calculation for SRIM simulation was monolayer collision steps/surface sputtering and, as the Ar ion energy, 1.2 keV was used. Specific simulation conditions are described in Table II.

3. RESULTS AND DISCUSSION

The use of focus ring in the reactive ion etch system improves etch uniformity by extending the plasma over the wafer surface and by focusing the electric field within the focus ring.[30] However, as mentioned earlier, due to the continuous reactive ion bombardment during the etching, the focus ring is damaged and eroded. Especially, as shown in Figure 3(a), when the focus ring height is located higher than wafer height, the plasma sheath height for the focus ring is higher than the plasma sheath on the wafer surface and the edge of the focus ring is intensively bombarded by the reactive ions. When the edge of the focus ring is damaged and eroded by continuous and intensive reactive ion bombardment, the uniformity of the plasma near the edge of the wafer is changed and the number of particles is increased significantly, then, the focus ring has to be replaced with a new focus ring.

The focus ring is bombarded by the ion accelerated by the sheath potential developed on the focus ring surface. When the same 12.56 MHz bias power is applied to the substrate, and when the same bias voltage V_o is applied to the substrate, depending on the capacitance of the focus ring, the sheath voltage (V_{p1} or V_{p2}) formed on the focus ring can be changed. If one material with the capacitance C is used as shown in Figure 3(b), the sheath voltage on the focus ring will be as follows;

$$Q = C_{p1}V_{p1} = CV \tag{1}$$

$$V_o = V_{p1} + V \tag{2}$$

$$V_{p1} = C/(C_{p1} + C) \times V_o \tag{3}$$

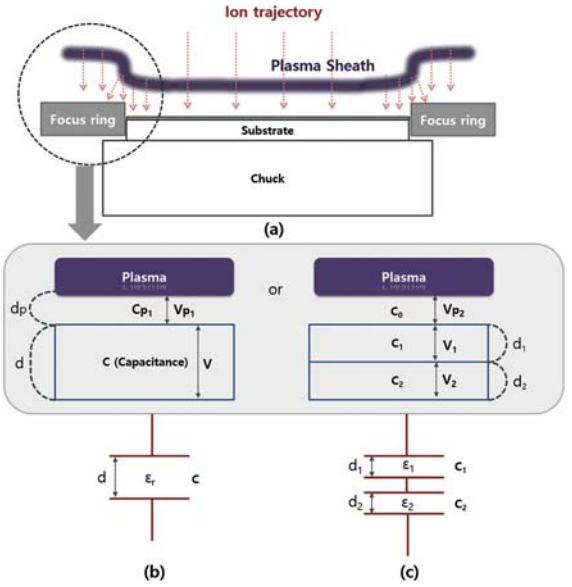

Fig. 3. Schematic diagram showing the control of the plasma sheath voltage on a focus ring by varying the capacitance of the focus ring material. (a) side view of the plasma sheaths on the wafer and focus ring. Plasma sheath and capacitance of focus ring (b) when one material was used and (c) when a multilayer material was used as the focus ring material to change the capacitance of the focus ring.

Therefore, the sheath potential V_{p1} is related to the capacitance (C) of the focus ring material and the smaller capacitance will give smaller sheath voltage on the focus ring, which is more beneficial in decreasing the etch rate of focus ring by decreasing reactive ion bombardment energy. The decrease of the materials capacitance can be achieved by using the material with smaller dielectric constant from the following equation;

$$C = \varepsilon_0 \varepsilon_r \frac{A}{d} \tag{4}$$

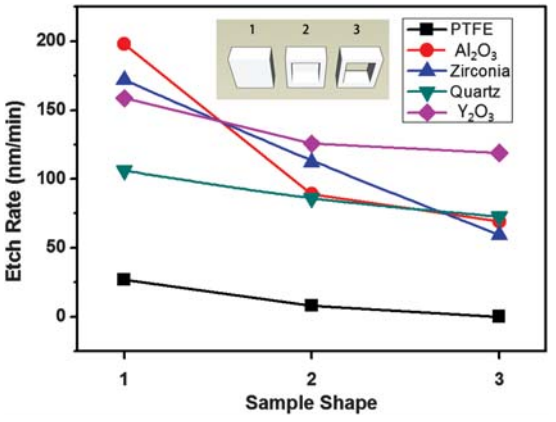

Fig. 4. Etch rates of SiO_2 located on the top of focus ring fabricated with various materials and various structures in Figure 2.

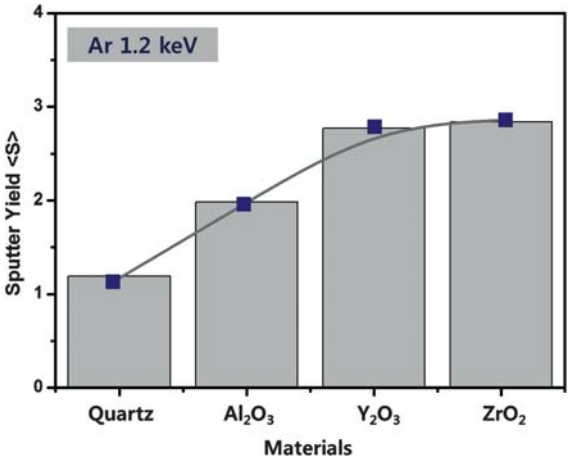

Fig. 5. Comparison of sputter yield with various dielectric materials using SRIM simulation.

where, ε_0 is the permittivity for air $= 8.854 \times 10^{-12}$ F·m^{-1} and ε_r = relative permittivity (or dielectric constant), A is the area of the capacitor, and d is the distance between two electrodes of the capacitor. However, materials with lower dielectric constant are generally soft and easily etched by the reactive ions. Therefore, when lower dielectric constant materials are used as the focus ring material, even though the sheath potential on the focus ring can be decreased, that is, the reactive ion bombardment energy can be decreased, due to the higher etch reactivity and high sputter yield, the focus ring is more easily damaged and eroded. Therefore, as shown in Figure 3(c), to improve the lifetime of the focus ring, two or multiple materials with different dielectric constants cladded in series may need to be used. By using the top material with the thickness d_1 with a low sputter yield and low reactivity to the etch gas and by using the bottom material with the thickness d_2 with a low dielectric constant including the air gap (because the air has the lowest dielectric constant of 1.0), not only the low reactive ion bombardment energy to the focus ring (that is, low sheath voltage on the focus ring) but also lower sputter etch and low etch reactivity of the focus ring surface material could be achieved.

Using five different materials such as PTFE, Al_2O_3, ZrO_2, quartz, and Y_2O_3 with three different structures shown in Figure 2 as the focus ring body, glass substrates deposited with SiO_2 were located on the top of the focus ring body, the etch experiment was carried out and the results on the SiO_2 etch rates for different materials and structures are shown in Figure 4. To etch SiO_2, 800 W of 13.56 MHz ICP source power, 1200 W of 12.56 MHz rf power, 75 mTorr of operating pressure, and the gas mixture of Ar (200 sccm)/CF_4 (45 sccm)/O_2 (30 sccm) were used. As shown in Figure 4, among the various materials, PTFE which has the lowest dielectric constant among the investigated five materials exhibited the lowest SiO_2 etch rate due to the lowest sheath voltage formed on the material surface. Also, quartz material which has the second lowest dielectric constant exhibited the second lowest etch

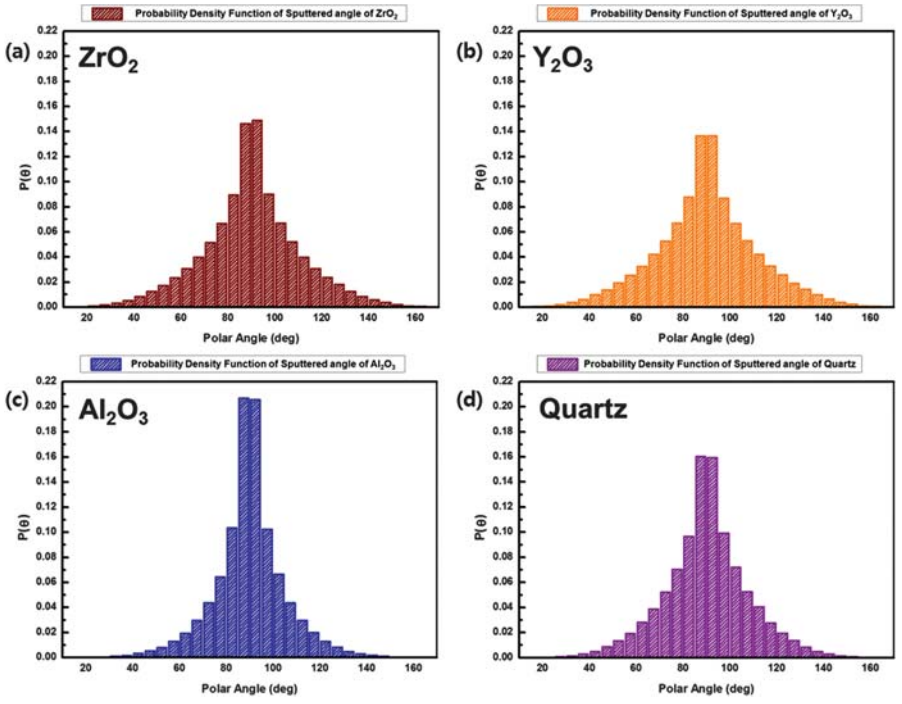

Fig. 6. Probability density function of dielectric materials sputtered by Ar atom using SRIM simulation.

rate. In the case of other materials, due to the high enough capacitances, the differences in the plasma sheath voltage may not be significantly different, therefore, no significant differences in SiO_2 etch rates could be observed. In the case of different structures, as shown in Figure 4, instead of solid material, the structure with more air gap exhibited the lower SiO_2 etch rates due to the overall lower dielectric constant by including air gap in the structure. In fact, in the case of sample shape 3, all of the inside area is air gap, but, due to the sidewall structure of the material, the overall dielectric constant was also affected by the material body, therefore, the etch rates were also affected by the material itself. Therefore, from this experiment, it can be concluded that, by using the focus ring material/structure to have the lowest dielectric constant, the sheath voltage on the focus ring is decreased and the reactive ion bombardment energy to the focus ring can be decreased. SRIM simulation in Figure 5 gives more information on the materials sputtered by Ar bombardment from the surface.

Figure 6 shows the probability density function of sputtered atom from the surface of dielectric material after 1.2 keV Ar bombardment. Ar particle was bombarded to the normal direction of the surface. As shown in Figure 6, the focus ring material sputtered off from the surface was distributed at the wider angle in the sequence of Al_2O_3 (narrower), quartz, ZrO_2, and Y_2O_3 (wider) similar to the sequence of the sputter yield as shown in Figure 5. Therefore, when SiO_2 or Al_2O_3 are used as the top material of the focus ring, especially for the sputter etching, it is believed that, it will have the least chance to have the sputtered material to be redeposited on the wafer surface which could reduce the problems related to the particle generation by the focus ring.

4. CONCLUSION

The material and structure of the focus ring, which is required for the nanoscale semiconductor etch processes for etch uniformity, have been investigated to increase the lifetime of the focus ring by considering the capacitance (dielectric constant) of the material on the ion energy bombarding the focus ring surface. Instead of using focus ring material with high dielectric constant, by using the focus ring material with low dielectric constant, the ion bombardment energy to the focus ring can be decreased while keeping the same sheath voltage to the wafer during the etching. Among the five different materials having different dielectric constants such as polytetrafluoroethylene (PTFE), alumina (Al_2O_3), zirconia (ZrO_2), quartz (SiO_2), and yttrium oxide (Y_2O_3), the PTFE which has the lowest dielectric constant exhibited the lowest etch rate of the focus ring due to the lowest sheath voltage. Also, for all the materials, the focus ring structure with more air gap exhibited less etch rates also due to the overall smaller dielectric constant of the material. However, in general, the material with the lower dielectric constant tends to have higher sputter yield and higher reactivity with etch gases. Therefore, instead of using a single solid material as the focus ring material, by using a multilayer cladded focus ring material which is composed of a top material having a low sputter yield and low etch reactivity and a bottom materials having a low dielectric constant (including air gap which has the lowest dielectric constant of 1.0), it is believed that, the lifetime of the focus ring can be significantly improved, and which decreases the process variation and particle issue during the nanoscale semiconductor processing. The results were also confirmed by SRIM simulation.

Acknowledgments: This study was supported by the NRF-2016M3A7B4910429 and also by SEMES cooperative research project supported in 2015.

References and Notes

1. H. Abe, Y. Masahiro, and N. Fujiwara, *Jpn. J. Appl. Phys.* 47, 1435 (**2008**).
2. I. Chun, A. Efremov, G. Y. Yeom, and K. H. Kwon, *Thin Solid Films* 579, 136 (**2015**).
3. T. Yagisawa, T. Shimada, and T. Makabe, *J. Vac. Sci. Technol. B* 23, 2212 (**2005**).
4. N. Y. Babaevaa and M. J. Kushnerb, *J. Appl. Phys.* 101, 113307 (**2007**).
5. Y. Uchida, Mounting table structure and method of holding focus ring, U.S. Patent 9,209,060, December (**2015**).
6. T. Panagopoulos, D. Kim, V. Midha, and D. J. Economou, *J. Appl. Phys.* 91, 2687 (**2002**).
7. M. Kubota and T. Shima, Focus ring, U.S. Patent 20,150,243,488, Auguest (**2015**).
8. M. E. Koltonski, Focus ring replacement method for a plasma reactor, and associated systems and methods, U.S. Patent 20,150,340,209, November (**2015**).
9. Y. Kobayashi, J. Watanabe, T. Okada, and T. Nara, Focus ring and manufacturing method therefor, U.S. Patent No. 9,196,512, November (**2015**).
10. K. Imafuku, Silicon focus ring, U.S. Patent 9,399,584, July (**2016**).
11. N. Y. Babaeva and M. J. Kushner, *J. Phys. D: Appl. Phys.* 41, 062004 (**2008**).
12. A. I. Kingon, J. P. Maria, and S. K. Streiffer, *Nature* 406, 1032 (**2000**).
13. K. Onisawa, M. Fuyama, K. Tamura, K. Taguchi, T. Nakayama, and Y. Ono, *J. Appl. Phys.* 68, 719 (**1990**).
14. S. Sayan, N. V. Nguyen, J. Ehrstein, T. Emge, E. Garfunkel, M. Croft, X. Zhao, D. Vanderbilt, I. Levin, E. P. Gusev, H. S. Kim, and P. J. McIntyre, *Appl. Phys. Lett.* 86, 152902 (**2005**).
15. S. K. Garg, H. Kilp, and C. P. Smyth, *J. Chem. Phys.* 43, 2341 (**1965**).
16. L. G. Hector and H. L. Schultz, *J. Appl. Phys.* 7, 133 (**1936**).
17. D. F. Filipovic, S. S. Gearhart, and G. M. Rebeiz, *IEEE Trans. Microwave Theory Tech.* 41, 1738 (**1993**).
18. J. Robertson, *Rep. Prog. Phys.* 69, 327 (**2006**).
19. K. Endo and T. Tatsumi, *Appl. Phys. Lett.* 68, 2864 (**1996**).
20. Y. Zhou, K. Hirao, Y. Yamauchi, and S. Kanzaki, *J. Euro. Ceram. Soc.* 24, 3465 (**2004**).
21. C. Degueldre, S. Conradson, and W. Hoffelner, *Comput. Mater. Sci.* 33, 3 (**2005**).
22. X. Li and B. Hafskjold, *J. Phys.: Condens. Matter.* 7, 1255 (**1995**).
23. P. Mondal, A. Klein, W. Jaegermann, and H. Hahn, *Solid State Ionics* 118, 331 (**1999**).

24. K. E. Sickafus, H. Matzke, T. Hartmann, K. Yasuda, J. A. Valdez, P. Chodak III, M. Nastasi, and R. A. Verrall, *J. Nucl. Mater.* 274, 66 **(1999)**.
25. M. J. Pellin, R. B. Wright, and D. M. Gruen, *J. Chem. Phys.* 74, 6448 **(1981)**.
26. M. Shayesteh and R. Duffy, *IEEE Trans. Semicond. Manuf.* 28, 508 **(2015)**.
27. M. C. Santos, D. W. Miwa, and S. A. S. Machado, *Electrochem. Commun.* 2, 692 **(2000)**.
28. B. Q. Han and D. C. Dunand, *Mater. Sci. Eng. A* 277, 297 **(2000)**.
29. G. Busker, A. Chroneos, and R. W. Grimes, *J. Am. Ceram. Soc.* 82, 1553 **(1999)**.
30. L. Tong, *Jpn. J. Appl. Phys.* 54, 06GA01 **(2015)**.

Received: 30 March 2016. Accepted: 5 September 2016.